




Primary role of the Tol-Pal complex in bacterial outer membrane lipid homeostasis

Received: 4 September 2024

Accepted: 24 February 2025

Published online: 07 March 2025

Wee Boon Tan ^{1,2} & Shu-Sin Chng ^{1,2} 

Gram-negative bacteria are defined by an outer membrane (OM) that contributes to envelope integrity and barrier function. Building this bilayer requires proper assembly of lipopolysaccharides, proteins, and phospholipids, yet how the balance of these components is achieved is unclear. One system long known for ensuring OM stability is the Tol-Pal complex, which has been implicated in maintaining OM lipid homeostasis. However, assignment of Tol-Pal function has been challenging, owing to its septal localization and associated role(s) during division. Here, we uncouple the function of Tol-Pal in OM lipid homeostasis from its impact on cell division in *Escherichia coli*, by engineering a chimeric complex that loses septal enrichment. We demonstrate that this peripherally-localized Tol-Pal complex is fully capable of maintaining lipid balance in the OM, thus restoring OM integrity and barrier. Our work establishes the primary function of the Tol-Pal complex in OM lipid homeostasis, independent of its role during division.

The unique feature of the Gram-negative bacterial cell envelope is the presence of the outer membrane (OM). This asymmetric lipid bilayer is essential for growth and confers protection against external insults, including antibiotics. Lipopolysaccharides (LPS) are packed tightly together in the outer leaflet to impede permeability, while phospholipids (PLs) predominantly occupy the inner leaflet^{1–3}. The OM also contains abundant β -barrel proteins forming channels that allow selective passage of solutes across the bilayer⁴. Notably, lipid-mediated interactions may facilitate the lateral clustering of OM proteins (OMPs) into islands that are extensively found throughout the OM^{5,6}. Consequently, the stability and barrier function of the OM depends acutely on the proper assembly of LPS, PLs, OMPs, and even lipoproteins, at optimal levels to achieve homeostasis. Furthermore, the OM is tethered to the peptidoglycan cell wall to maintain overall structural integrity and stability of the entire cell envelope^{7–9}.

The transport and assembly of LPS, OMPs, and lipoproteins into the OM are relatively well-characterized^{1,4,10}. These processes are known to be unidirectional, making it a challenge for the cell to directly adjust the levels of LPS, OMPs, and lipoproteins post-assembly. In contrast, PL transport is bidirectional^{11–13}. This feature may facilitate the fine control of PL levels at the OM relative to other components, possibly allowing the maintenance of a stable membrane^{3,14}. Unfortunately, the processes

that move PLs between the two membranes are still poorly understood. The machines that mediate anterograde (IM-to-OM) transport of bulk PLs have remained elusive until recently, where three collectively essential AsmA family proteins, YhdP, TamB, and YdbH, are now implicated in the process^{15–17}. The OmpC-Mla system is known to transport PLs that have mislocalized to the outer leaflet of the OM back to the IM¹⁸, yet whether it has any major impact on overall OM stability is unclear. In fact, another system, the Tol-Pal complex, has also been implicated in retrograde (OM-to-IM) transport, but of bulk PLs¹⁴. Unlike cells lacking OmpC-Mla, those lacking the Tol-Pal complex exhibit excess PL build-up at the OM, directly altering PL and LPS balance, and display a slower measured rate of movement of OM PLs back to the IM¹⁴. In this regard, the Tol-Pal complex may be a key player in maintaining OM integrity and stability via lipid homeostasis.

The Tol-Pal complex is highly conserved and comprises five proteins^{19–24}. TolQ, TolR, and TolA are integral membrane proteins that form a proton motive force (pmf)-utilizing subcomplex at the IM²⁵. Pal is an OM lipoprotein that can bind the periplasmic protein TolB or peptidoglycan (but not simultaneously)^{26–28}, with the latter interaction contributing to OM-cell wall tethering^{27,29,30}. Strains lacking any Tol-Pal component are known to have pleiotropic OM defects, including hypersensitivity to detergents and antibiotics, leakage of periplasmic

¹Department of Chemistry, National University of Singapore, Singapore. ²Singapore Center for Environmental Life Sciences Engineering, National University of Singapore (SCELSE-NUS), Singapore, Singapore. ✉e-mail: chmchngs@nus.edu.sg

contents, and OM vesiculation^{20,31–34}. These phenotypes indicate substantial perturbations to envelope integrity, which is consistent with lipid dyshomeostasis observed in the OM^{14,33,35}. The definitive assignment of Tol-Pal function is confounded, however, by the fact that $\Delta tol\text{-}pal$ mutants also exhibit division phenotypes, specifically cell chaining in extreme osmolality^{36,37}. It is believed that the lack of Tol-Pal causes delayed OM invagination^{36,38}, and most recently, also cell wall remodeling and separation defects³⁹. Notably, all components of the Tol-Pal complex localize to the cell septum during division^{36,38,40,41}. Septally localized TolQRA facilitates the recruitment of TolB and Pal to the division site^{38,40}, where pmf-induced conformational changes in TolA are thought to transmit a pulling force on TolB. Consequently, TolB-Pal interaction can be perturbed, leading to the dynamic enrichment of Pal-peptidoglycan binding, believed to be required for proper OM invagination at mid-cell. While TolQRA is also thought to regulate cell wall biosynthesis⁴², it is not clear how enrichment of the Tol-Pal complex at the division site may ultimately modulate peptidoglycan remodeling, and impact cell separation. It is also unclear if and how septal-localized Tol-Pal contributes to OM lipid homeostasis. Yet, the involvement of Tol-Pal in both pathways is evident from synthetic genetic interactions between the *tol-pal* locus and genes involved in either cell wall remodeling or OM biogenesis³⁴. Interestingly, alleviating cell wall separation and division defects in *tol-pal* mutants does not appear to rescue OM instability³⁹. Given the complex phenotypes, teasing out the exact function(s) of Tol-Pal in these two seemingly independent processes has been challenging.

One approach to uncouple the role of the Tol-Pal complex in OM lipid homeostasis from cell division would be to prevent septal localization. Since PLs occupy the entire inner leaflet of the OM, it is possible that the Tol-Pal complex remains functional all around the cell envelope, in its proposed role in retrograde PL transport¹⁴. To test this idea, we explore the possibility of a chimera complex based on the known cross-compatibility between TolQR-TolA and the homologous ExbBD-TonB system. Like TolQRA, ExbBD uses the pmf to induce conformational changes in TonB to exert a mechanical pulling force, but on TonB-dependent transporters for metal/siderophore uptake^{43–46}. Both systems are also hijacked by bacteriocins for cell entry. Even though ExbBD-TonB does not display a preference for the septal region⁴⁷, some degree of cross-complementation has been reported between ExbBD and TolQR^{48–52}, indicative of possible interchangeability across the IM subcomplexes. In this work, we engineer a chimeric version of TonBTM-TolA that can work with the ExbBD subcomplex in *Escherichia coli*, giving rise to an assembled IM complex that no longer localizes specifically to the cell division site. We show that cells only expressing this peripherally localized complex still display defects in the division. Importantly, the ExbBD-TonBTM-TolA complex is fully functional in maintaining OM lipid homeostasis, in a manner dependent on TolB and Pal. Our work establishes that the primary function of the Tol-Pal complex is to mediate OM lipid homeostasis in Gram-negative bacteria.

Results

A TonBTM-TolA fusion retains the functionality of TolA in maintaining OM integrity but not cell division in a manner dependent on ExbBD

We hypothesized that Tol-Pal maintains OM integrity, presumably via retrograde PL transport, and this function does not require septal localization. To test this idea, we sought to engineer a TonBTM-TolA chimera that works with the ExbBD complex instead of TolQR. Notably, the ExbBD-TonB complex is not recruited to the division site⁴⁷, therefore the ExbBD-TonBTM-TolA variant may lose septal localization yet retain TolA function (Fig. 1a). Since TolA or TonB primarily interacts with TolQR or ExbBD, respectively, via its N-terminal transmembrane helix, we replaced the transmembrane helix of TolA with that of TonB. In this TonBTM-TolA chimera, the first 34 residues of TonB are fused to

the periplasmic domains of TolA (35–421 a.a.) (Fig. 1b). To assess its function in OM integrity, we expressed this construct in an MG1655 $\Delta tolQRA$ background strain, and examined SDS/EDTA or vancomycin sensitivity. Additional copies of ExbBD were expressed in trans in this mutant, as well as all control strains, to ensure sufficient ExbBD proteins available for both native TonB and TonBTM-TolA. As expected, the $\Delta tolQRA$ strain was extremely sensitive to SDS/EDTA and vancomycin. Remarkably, we found that the presence of the TonBTM-TolA fusion protein conferred strong resistance to both insults, indicating a fully restored OM barrier (Fig. 2a, b). In contrast, wild-type TolA only marginally rescued the barrier defects when expressed at comparable levels (Fig. S1). These observations are not unexpected, given that ExbBD is only known to weakly complement the absence of TolQR^{48,49,53}, and presumably less able to complex with TolA. Nevertheless, the striking difference between TonBTM-TolA and TolA highlights the importance of the TonB transmembrane helix (to effectively complex with ExbBD). Mutants lacking functional Tol-Pal also leak periplasmic contents, including RNase I, as indicated by the presence of RNA-degrading activity in culture supernatants (Fig. 2c). Expression of the TonBTM-TolA construct fully prevented RNase I leakage (Fig. 2c), further confirming that the chimera protein effectively replaces the role of TolA in maintaining OM integrity and barrier function.

Since TolQ and TolR were absent in this strain, the recovery of Tol-Pal OM function must be derived from an ExbBD-TonBTM-TolA complex. Consistently, when the chromosomal copy of *exbD* was removed, TonBTM-TolA no longer conferred SDS/EDTA and vancomycin resistance in $\Delta tolQRA$ (Fig. S2). Furthermore, a mutation (H20A) within the transmembrane helix of TonB, known to affect ExbBD-TonB complex formation and pmf utilization^{54–56}, fully abolished the ability of TonBTM-TolA to maintain OM barrier function (Fig. S2). To date, all reported functions of Tol-Pal require every component of the complex (TolQ, TolR, TolA, TolB, and Pal) to be present; thus, we checked if the ExbBD-TonBTM-TolA chimera complex requires TolB and Pal using a $\Delta tolQRA$ -*tolB-pal* ($\Delta tol\text{-}pal$) deletion strain. In this background further lacking TolB and Pal, TonBTM-TolA was unable to restore OM barrier function (Fig. 2a, b), unless both TolB and Pal were complemented in trans (Fig. S3), confirming that the fusion protein is performing a native Tol-Pal function.

Next, we checked if the TonBTM-TolA chimera also retains TolA function during cell division. As previously reported³⁹, the $\Delta tolQRA$ mutant was sensitive to low osmolality media (LBON) at elevated temperatures (Fig. 2d), a phenotype associated with cell chaining division defects. Interestingly, expressing TonBTM-TolA did not rescue growth, nor fully prevent cell chaining defects, under this condition (Fig. 2d, e). Therefore, the ExbBD-TonBTM-TolA complex appears incapable of replacing TolQRA in septal cell wall remodeling and/or OM invagination. Importantly, TonBTM-TolA was still stably expressed in cells grown at the same elevated temperature, thus effectively restoring OM barrier function (Fig. S4). Overall, our findings demonstrate that the TonBTM-TolA fusion, in complex with ExbBD, is able to execute the native function of Tol-Pal in maintaining OM stability, but not in cell division processes.

The ExbBD-TonBTM-TolA chimera complex ‘loses’ septal localization and ability to enrich Pal at mid-cell

The inability of TonBTM-TolA to rescue cell division defects may be due to a lack of septal localization. To determine if this is true, we examined the cellular localization of an N-terminally sfGFP-tagged version of TonBTM-TolA. This sfGFP-TonBTM-TolA functioned similarly to the TonBTM-TolA construct (Fig. S5). As a control, we also made a sfGFP-TolA fusion (with native TolA transmembrane domain), which did not rescue $\Delta tolQRA$ phenotypes (like wild-type TolA (Fig. S1)), despite being expressed at similar levels compared to sfGFP-TonBTM-TolA (Fig. S5). In both WT and $\Delta tolQRA$ strains, sfGFP-TolA was strongly enriched at cell division sites as expected. In stark contrast,

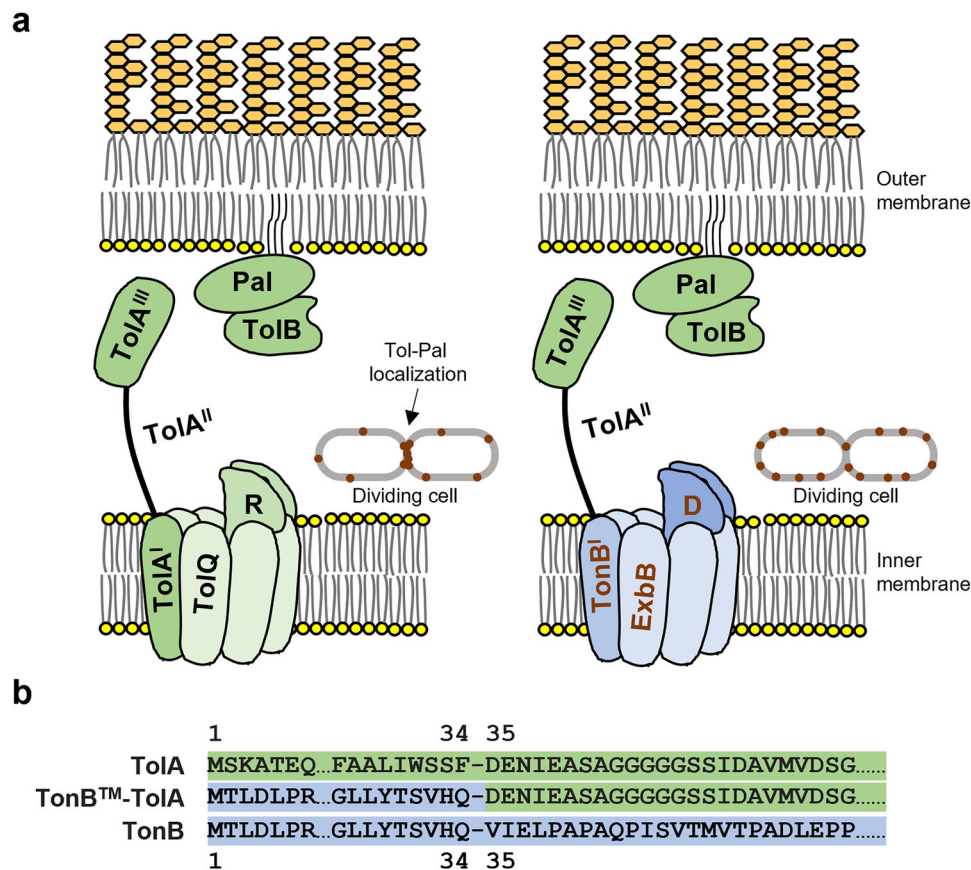


Fig. 1 | Preventing septal enrichment of the Tol-Pal complex using a TonBTM-TolA chimera. **a** Schematic representation of the native Tol-Pal complex (*left*) and the engineered chimeric complex (*right*), and their expected intracellular localization in dividing cells. Native Tol-Pal contains the TolQRA subcomplex at the IM, while the chimeric version contains instead a TonBTM-TolA fusion that works with ExbBD

in a subcomplex that is not recruited to the division site. TolB and Pal remain the same in both scenarios. **b** Design of the TonBTM-TolA fusion protein. The TonBTM-TolA construct contains the first 34 amino acids from the N-terminus of TonB, including its transmembrane helix, fused directly to the periplasmic domains of TolA (amino acid 35-421).

sfGFP-TonBTM-TolA did not localize specifically to the cell septum but was randomly distributed around the cell periphery of both background strains (Fig. 3a–c). Therefore, forcing TonBTM-TolA to interact with ExbBD prevents septal localization.

TolQRA is believed to dislodge TolB for Pal enrichment at the septum³⁸, therefore, we also investigated Pal localization in the presence of the ExbBD-TonBTM-TolA complex. Here, we expressed sfGFP-TonBTM-TolA and ExbBD in a previously reported $\Delta tolQR$ strain that also produces a functional Pal-mCherry fusion (from the native *tol-pal* locus)⁴⁰. In the WT background, Pal-mCherry was enriched at division sites due to the presence of functional TolQRA (Fig. 4a–c). In the $\Delta tolQR$ background, accumulation of septal Pal-mCherry was largely abolished, as others have observed⁴⁰. Remarkably, we demonstrated that the presence of the ExbBD-TonBTM-TolA complex did not restore septal Pal enrichment (Fig. 4); we conclude that the observed cell division defects (Figs. 2d, e, S2, S4) in strains expressing ExbBD-TonBTM-TolA were due to loss of septal-localized Tol-Pal function. Given that OM barrier functions are fully restored, we believe that the ExbBD-TonBTM-TolA complexes localized peripherally are sufficient to perform the function of Tol-Pal in OM stability and homeostasis.

An unexpected observation in our microscopy studies was that expressing ExbBD-TonBTM-TolA actually rescued the mild morphological defects seen in the above $\Delta tolQRA$ and $\Delta tolQR$ strains grown under normal osmolality conditions (Figs. 5 and S6). Disruption of Tol-Pal function is known to cause a moderate increase in cell width, giving rise to “fatter” cells^{33,36}, a morphological change previously attributed

to defects in cell division. Since restoring OM integrity alone in these strains returned cell width back to normal, it is likely that this cell morphological defect arises from OM lipid dyshomeostasis in *tol-pal* mutants.

Peripherally localized ExbBD-TonBTM-TolA complex retains Tol-Pal function in OM lipid homeostasis

tol-pal mutants are known to release excess amounts of OM vesicles (OMVs) relative to WT^{20,33}, especially from the septum; this hypervesiculation phenotype is believed to be associated with both the loss of septal peptidoglycan-OM tethering, as well as OM instability and lipid dyshomeostasis. Since ExbBD-TonBTM-TolA rescues OM defects, we wondered if OM hypervesiculation was alleviated. Following [¹⁴C]-acetate labeling of cellular lipids, we isolated and quantified OMVs from culture supernatants of WT and $\Delta tolQRA$ strains expressing ExbBD and TonBTM-TolA. Interestingly, while $\Delta tolQRA$ mutant produced ~50-fold more OMVs than WT, the presence of ExbBD-TonBTM-TolA reduced that excess by ~79% (i.e., only ~10-fold more than WT) (Fig. 6a). This residual OM vesiculation is likely due to the lack of Tol-Pal function at the division site, manifesting as problems in OM invagination. Importantly, it appears that peripherally localized Tol-Pal function is sufficient to reduce OM hypervesiculation significantly, highlighting OM instability and lipid dyshomeostasis as the main contributors to this phenotype in *tol-pal* mutants.

We went on to ascertain if ExbBD-TonBTM-TolA indeed restored OM lipid homeostasis, thereby rescuing OM barrier defects and

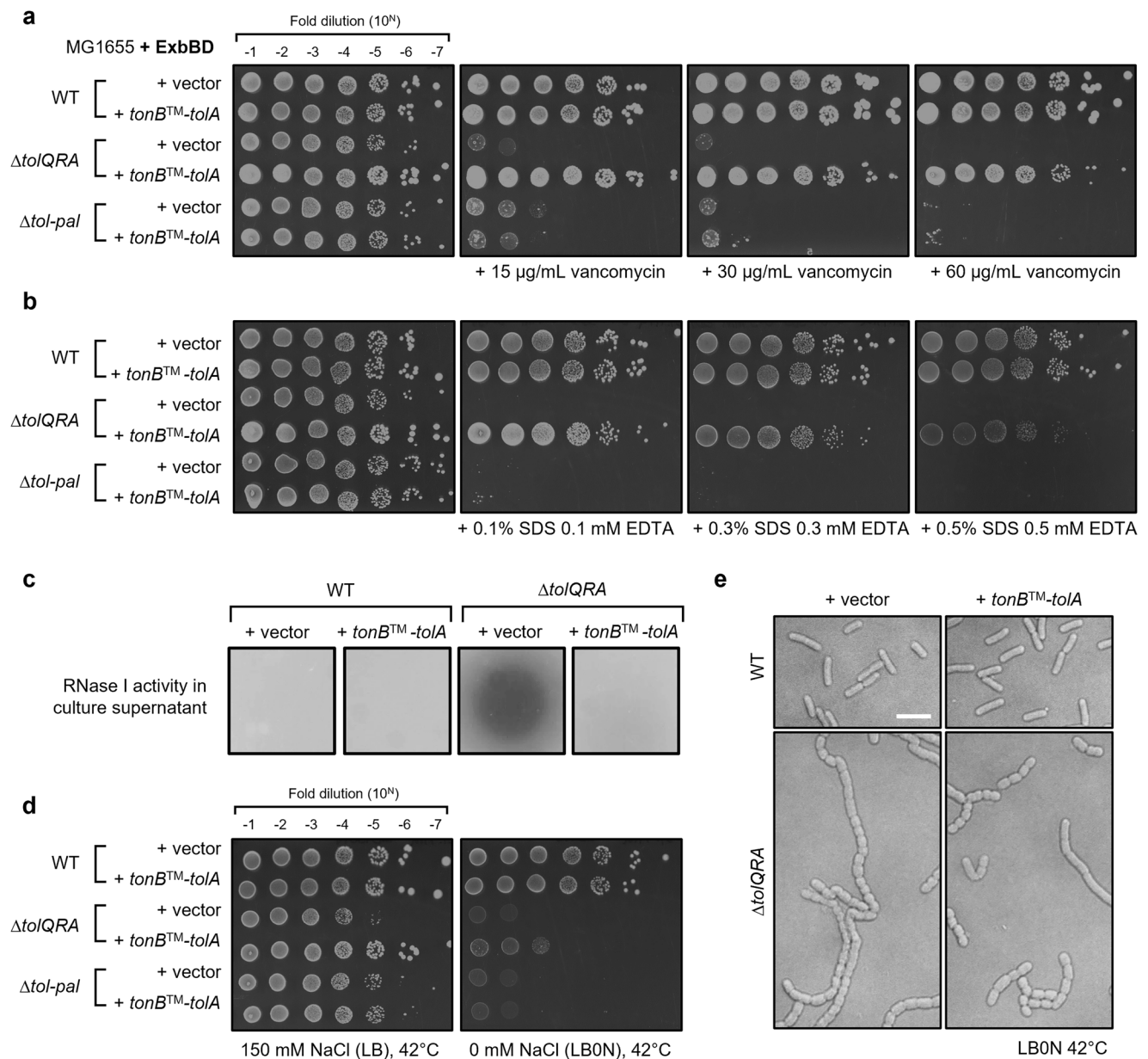


Fig. 2 | Chimeric ExbBD-TonBTM-TolA preserves the function of TolQRA for outer membrane integrity but not cell division. a, b Efficiency of plating (EOP) of MG1655 wild-type (WT), $\Delta tolQRA$, and $\Delta tol-pal$ strains, containing either the pET23/42 empty vector⁷⁰ or the plasmid expressing TonBTM-TolA, on LB agar plates supplemented with **a** vancomycin or **b** SDS/EDTA at the indicated concentrations at 37 °C. **c** RNase leakage assay of the WT and $\Delta tolQRA$ strains expressing TonBTM-TolA chimera, as judged by degradation of RNA (halo formation) when filtered culture supernatants were spotted on agar containing yeast RNA. **d** EOP of the same strains

in **a, b** on either normal LB (150 mM NaCl) or LB0N (no NaCl) agar at 42 °C. **e** Differential interference contrast (DIC) microscopy images of WT and $\Delta tolQRA$ strains expressing TonB-TolA chimera grown in LB0N media at 42 °C. Scale bar represents 5 μ m. Cropped images shown are representative of at least three different uncropped field-of-views. All strains used here express additional copies of ExbBD from a pBAD33 vector⁷¹ to enhance ExbBD-TonBTM-TolA chimera complex formation, and to avoid depletion of ExbBD for its native TonB-dependent function.

hypervesiculation. Mutants lacking the Tol-Pal complex accumulate excess PLs in the OM, reflected in an elevated PL:LPS ratio¹⁴. This PL excess presumably gives rise to perturbation in OM lipid asymmetry, where PLs mislocalize to the outer leaflet, providing substrates for hepta-acylation of LPS by PagP¹⁴. Expectedly, in [³²P]-radiolabeled lipid profiling experiments, the $\Delta tolQRA$ mutant exhibited increased PL:LPS ratio and hepta-acylated LPS levels, as previously reported (Fig. 6b, c). Remarkably, we demonstrated that expression of TonBTM-TolA reversed both molecular phenotypes back to levels similar to WT, effectively re-establishing OM lipid homeostasis. Taken together, we conclude that the Tol-Pal complex can mediate OM lipid homeostasis without enrichment to the division site. Maintaining OM

stability and homeostasis is the primary function of the Tol-Pal complex.

Discussion

The Tol-Pal complex is functionally involved in cell division and in OM lipid homeostasis. In this work, we have demonstrated that the Tol-Pal complex performs its function in OM homeostasis independent of its roles during cell division. We have engineered a chimeric protein, with the transmembrane domain of TonB fused to the periplasmic “effector” domains of TolA, that forms a functional complex with ExbBD instead of TolQR. This ExbBD-TonBTM-TolA complex itself does not localize, hence cannot enrich Pal, to the septum (Figs. 3 and 4),

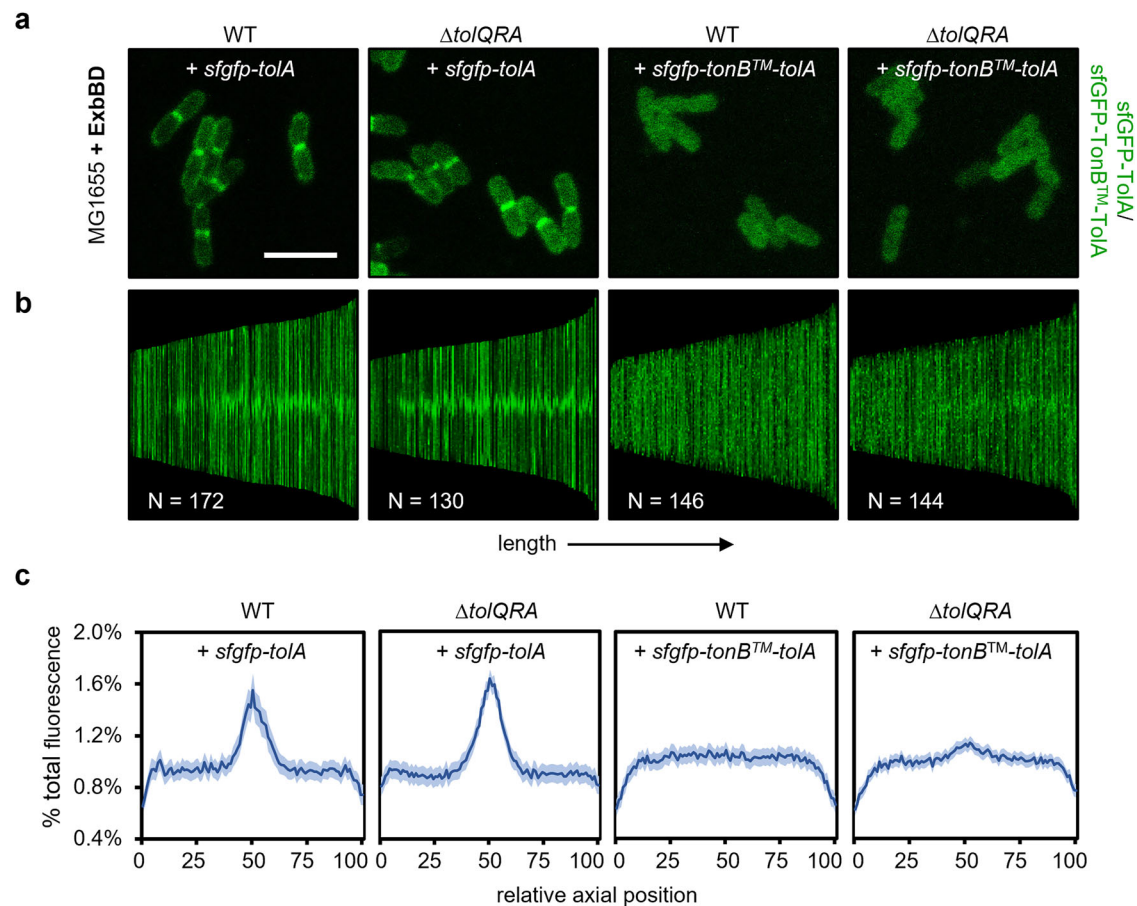


Fig. 3 | TonBTM-TolA is not spatially enriched at the cell septum. **a** Fluorescence microscopy images of MG1655 WT and $\Delta tolQRA$ strains, expressing sfGFP-TolA or sfGFP-TonBTM-TolA from pET23/42. Scale bar represents 5 μ m. Cropped images shown are representative of at least three different uncropped field-of-views.

b Demographic representations of the sfGFP-TolA or sfGFP-TonBTM-TolA fluorescence signals in the indicated strains measured and normalized along the long axis

of individual cells, sorted according to cell length, and aligned to mid-cell.

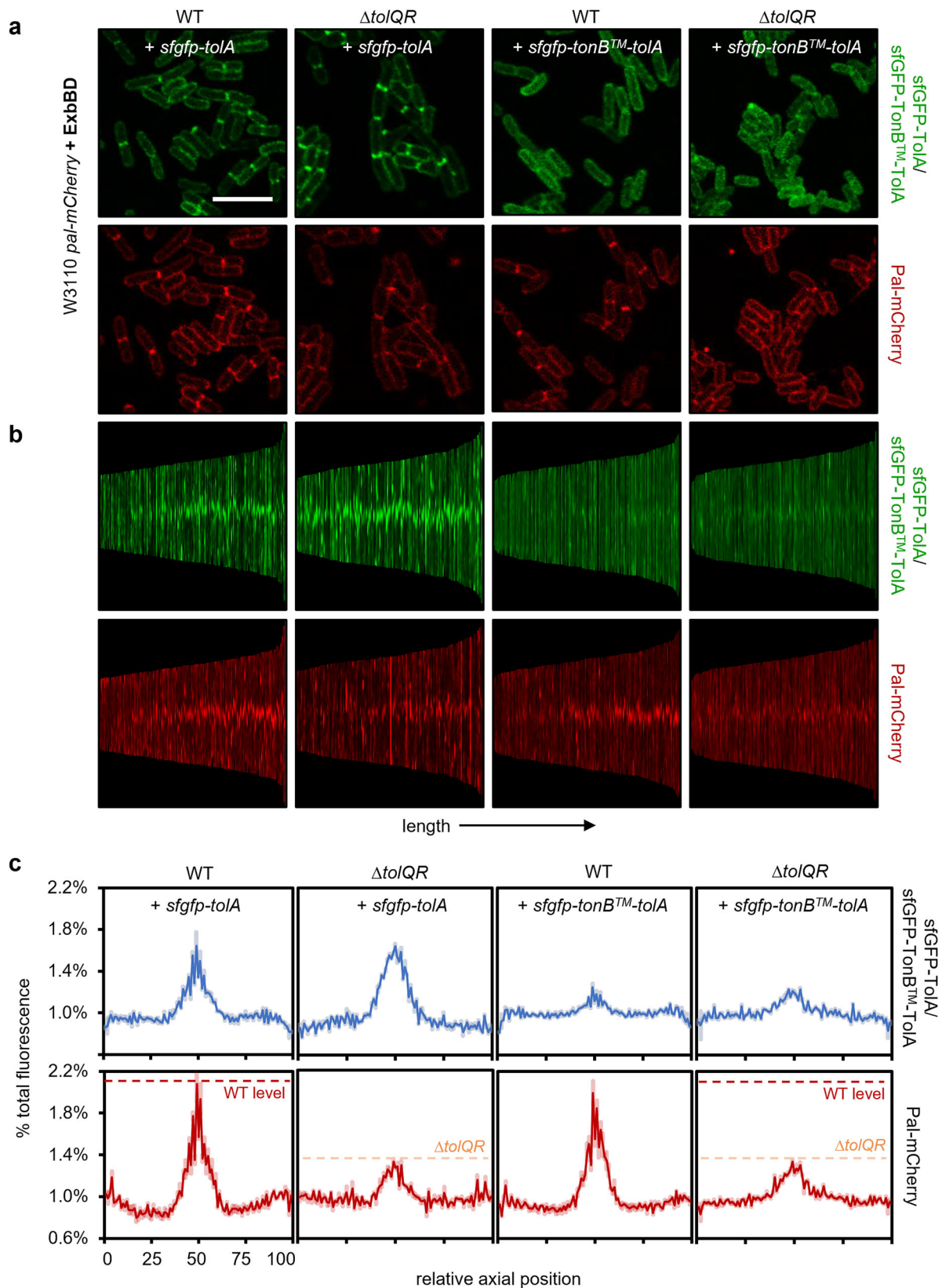
c Average percentage distribution of the sfGFP-TolA or sfGFP-TonBTM-TolA fluorescence signals along the long axis of all cells measured in **b**, where the relative axial position of 50 corresponds to mid-cell (septum), and 1 and 100 correspond to the poles, respectively. 95% confidence intervals are shown. All strains here express additional copies of ExbBD from a pBAD33 vector.

resulting in the loss of cell division function(s) associated with the Tol-Pal complex (Fig. 2d, e). Yet, this peripherally distributed chimera complex retains the function of Tol-Pal in maintaining OM lipid homeostasis (Fig. 6), thus restoring OM stability and permeability barrier function (Fig. 2a–c). Our work establishes that OM defects in *tol-pal* mutants are not indirect consequences of problem(s) that arise during cell division and favors a model where the Tol-Pal complex plays a primary role in maintaining OM lipid homeostasis throughout the cell.

The physiological function of the Tol-Pal complex has been a longstanding question in the field. As early as the 1960s, the Tol-Pal complex was thought to be important for OM stability^{19–21,32,57,58}. Strains lacking any of the Tol-Pal proteins release more OMVs and exhibit exacerbated OM permeability defects. Yet, it was also known that *tol-pal* mutants display cell chaining defects, but only under extreme osmolality conditions^{36,37}. Therefore, it has been challenging to interpret such pleiotropic phenotypes and assign the real function of the Tol-Pal complex. In 2007, the Tol-Pal complex was reported to localize to the cell septum³⁶, highlighting a potential role during cell division, specifically to facilitate OM invagination. This idea quickly gained traction then^{38,42,59,60}, given that Tol-Pal is a trans-envelope complex, and that Pal tethers the OM to the peptidoglycan layer; there appears to be an underlying assumption that the OM and cell chaining phenotypes in *tol-pal* mutants were somehow due to defective OM constriction during cell division. A key development that challenges this

prevailing thought was the recent discovery of OM lipid dyshomeostasis in *tol-pal* strains^{14,35}, which can logically account for OM stability and permeability defects; it became less clear how defects in OM invagination can actually give rise to changes in lipid compositions in the OM. It is also now established that the cell chaining phenotype under low osmolality conditions is, in fact, due to defects in septal cell wall remodeling and separation³⁹. Notably, suppressing chaining phenotypes by overexpressing cell wall hydrolases did not significantly alleviate OM permeability and hypervesiculation defects in *tol-pal* strains³⁹. This is in agreement with OM phenotypes already manifesting in *tol-pal* strains grown under normal osmolality conditions where chaining is naturally suppressed. While it is unlikely that OM phenotypes are downstream of cell division defects in *tol-pal* mutants, it remained difficult to clarify true causal relationships. In this regard, we have now introduced a novel approach to uncouple the function of Tol-Pal in maintaining OM lipid homeostasis from its role(s) in cell division. By essentially preventing septal enrichment of a functional Tol-Pal complex, our strategy facilitates the definition of Tol-Pal function in OM lipid homeostasis, contributing to a critical advance in our understanding of this decades-old problem.

By separating the functions of the Tol-Pal complex in OM lipid homeostasis and cell division, we are also now able to explain most of the pleiotropic phenotypes observed in *tol-pal* mutants. OM permeability defects are a direct result of lipid dyshomeostasis. Interestingly, we have found that restoring OM lipid homeostasis was sufficient to



rescue the mild morphological defects, i.e. wider cells, observed in *tol-pal* strains grown under normal osmolality conditions (Fig. 5). Therefore, we reason that the wider cellular morphology is likely due to both decreased rigidity, and the increased surface area, of the OM, as a result of excess PL accumulation. Furthermore, it appears that OM hypervesiculation can also be largely attributed to lipid

dyshomeostasis. We have shown that expressing the functional peripheral Tol-Pal complex was able to reduce OMV shedding drastically (Fig. 6a), indicating that an unstable OM is indeed a major contributor to vesiculation in these cells. Overall, we deduce that defects in OM stability and permeability, hypervesiculation, and cellular morphology, in cells grown under normal osmolality, can be traced back to the

Fig. 4 | Peripherally localized ExbBD-TonBTM-ToIA complex no longer promotes septal enrichment of Pal. **a** Fluorescence microscopy images of W3110 WT (expressing Pal-mCherry from the native *pal* chromosomal locus) and the corresponding $\Delta tolQR$ strains, expressing sfGFP-ToIA (control) or sfGFP-TonBTM-ToIA. The scale bar represents 5 μ m. Cropped images shown are representative of at least three different uncropped field-of-views. **b** Demographic representations of the sfGFP-ToIA/sfGFP-TonBTM-ToIA (green) and Pal-mCherry (red) fluorescence signals

in the indicated strains measured and normalized along the long axis of individual cells, sorted according to cell length and aligned to mid-cell. **c** Average percentage distribution of the sfGFP-ToIA/sfGFP-TonB-ToIA (blue) and Pal-mCherry (scarlet) fluorescence signals along the long axis of all cells measured in **b**, where the relative axial position of 50 corresponds to mid-cell (septum), and 1 and 100 correspond to the poles, respectively. 95% confidence intervals are shown. All strains here express additional copies of ExbBD from a pBAD33 vector.

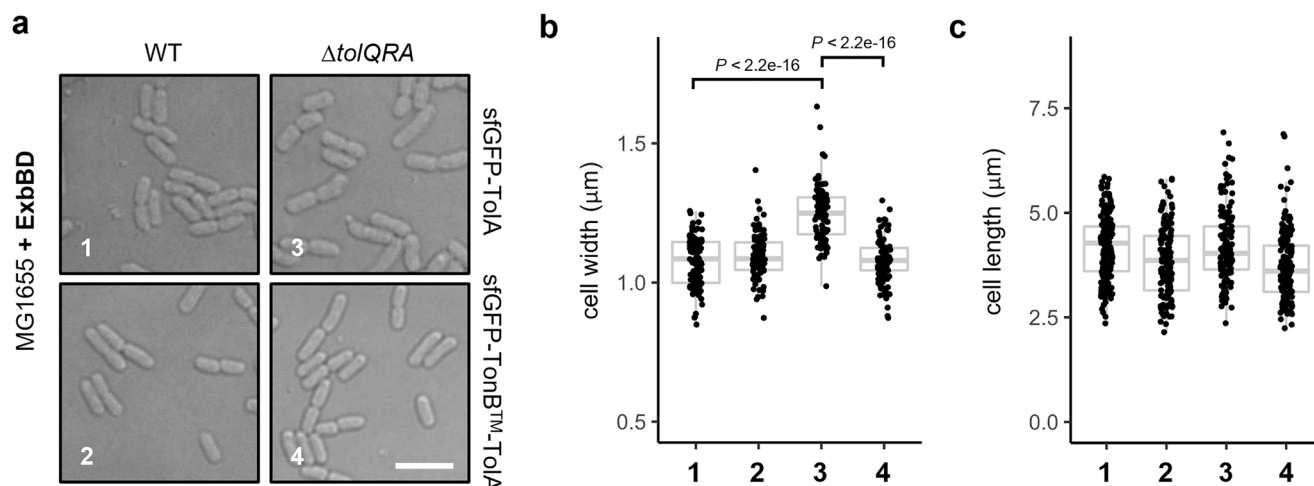


Fig. 5 | Cell morphological defects are restored by ExbBD-TonBTM-ToIA. **a** DIC microscopy images of MG1655 WT and $\Delta tolQRA$ strains, expressing sfGFP-ToIA or sfGFP-TonBTM-ToIA. Scale bar represents 5 μ m. Cropped images shown are representative of at least three different uncropped field-of-views. **b**, **c** Quantification of the cell **b** width and **c** length of >100 individual cells of the same strains (numbered) shown in **a**. $N = 100$ for data shown in **b**; $N = 172, 146, 130$, and 144 for data shown in

c for #1, #2, #3, and #4, respectively. Box plot defines the median (center) and 25th and 75th percentile (lower and upper hinge); the whisker represents the range excluding outliers (outlier defined by sample with value further than 1.5 interquartile-range from the corresponding hinge). A two-sided Wilcoxon ranked sum test was used to test for statistical significance. All strains here express additional copies of ExbBD from a pBAD33 vector.

primary role of the Tol-Pal complex in OM lipid homeostasis. Nonetheless, the Tol-Pal complex is still important for OM invagination during cell division. This conclusion is consistent with the residual OMV shedding present in cells with restored OM lipid homeostasis, but deficient in septal localization of Tol-Pal. However, it remains unclear if and how OM invagination defects may contribute to cell wall remodeling and chaining defects, observed only under extreme osmolality conditions. Given that changes in osmolality can exert additional stresses on the cell envelope, and notably also alter enzymatic activities of cell wall biosynthetic enzymes⁶¹, remodeling and chaining defects may be a manifestation of ensuing synthetic interactions within the stressed envelope.

How the Tol-Pal complex mediates OM stability throughout the cell is not clear. We have demonstrated that retaining Tol-Pal function in the cell periphery is sufficient to maintain OM lipid homeostasis, but the molecular mechanism(s) remains elusive. Given the known ability of Pal to bind peptidoglycan, it is natural to first consider Pal-mediated OM-cell wall tethering as the main activity of the Tol-Pal complex. However, other tethering proteins (e.g., Lpp, OmpA) exist at much higher abundance throughout the cell in *E. coli*^{7,9,62}, raising the question of how the lack of Pal-mediated tethering from the cell periphery would give rise to such severe OM defects observed in *tol-pal* mutants. Furthermore, removing only TolB, which is expected to increase Pal binding to cell wall²⁸, also does not alleviate the OM phenotypes. Alternatively, it may be that the more dynamic nature of this system contributes to OM stability, even when Tol-Pal function is peripherally distributed. TolQRA is believed to modulate the interaction between TolB and Pal, continually influencing the levels of Pal binding to the cell wall, particularly at the cell septum³⁸. Yet, diffusion kinetics of Pal in the cell periphery of non-dividing cells did not change appreciably in response to ToIA or TolB mutations that cause OM defects³⁸,

suggesting little correlation between Pal-cell wall binding dynamics and Tol-Pal function. Overall, we believe that OM-cell wall tethering mediated by Pal is unlikely the key activity to realize Tol-Pal function in OM stability and lipid homeostasis. Instead, on the basis of excess PL accumulation in the OM and slower intermembrane PL exchange, we have previously hypothesized that the Tol-Pal complex has a possible activity in retrograde transport of bulk PLs¹⁴. Since TolQRA harnesses the pmf for force generation across the cell envelope, in part to alter TolB-Pal interaction, speculative models for how this force can translate to PL transport activity have thus been proposed^{2,14}; these models include active shuttling of a yet-to-be-identified PL-binding protein, and even pulling of the IM and the OM together for potential hemifusion events. In these scenarios, it is conceivable that Pal binding to peptidoglycan, which occurs through *meso*-diaminopimelate (*mDAP*) recognition²⁹, maybe a way to locate non-crosslinked regions in the cell wall mesh for trans-envelope transport. Ultimately, the proposed activity of the Tol-Pal complex in retrograde PL transport will enable fine control of PL content relative to other OM components, thereby directly contributing to the overall stability and homeostasis of the OM. These ideas require further investigation.

Regardless of the molecular mechanism, however, the function of the Tol-Pal complex in OM lipid homeostasis is likely also beneficial during cell division. After all, the IM components TolQ, TolR, and ToIA are recruited to the septum via at least two independent ways linked to septal cell wall biosynthesis^{36,41,63}, indicating a possible evolutionary advantage for Tol-Pal function(s) to exist at mid-cell. It is believed that Pal-mediated tethering of the OM to the cell wall contributes to septal OM invagination. We further propose that changing lipid composition, i.e. membrane remodeling, would also be important for this process. Specifically, changes in PL content at the inner leaflet of the OM, possibly facilitated by retrograde PL transport, may modulate

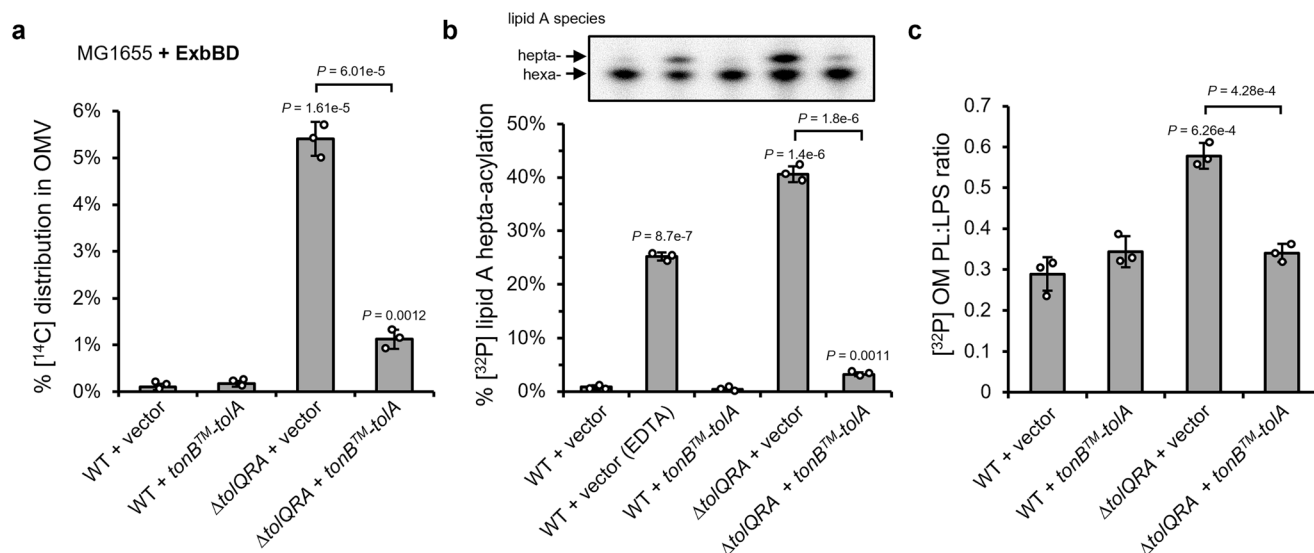


Fig. 6 | Peripherally localized Tol-Pal maintains outer membrane lipid homeostasis. **a** Quantification of OMV levels in MG1655 WT and $\Delta tolQRA$ strains expressing TonBTM-TolA, represented by levels of [¹⁴C]-labeled lipids in the filtered culture supernatant, relative to total [¹⁴C]-acetate labeling (cell pellet + OMV) of the respective strains. Data are presented as mean \pm standard deviation from three independent replicates. **b** Quantification of OM lipid asymmetry defects in WT and $\Delta tolQRA$ strains expressing TonB-TolA, represented by the levels of [³²P]-labeled hepta-acylated lipid A, following thin-layer chromatography (inset)/phosphor imaging analyses. PagP-mediated transfer of an acyl tail from outer leaflet PLs to

hexa-acylated lipid A serves as a proxy for lipid asymmetry in the OM. Data are presented as mean \pm standard deviation from three independent replicates. **c** Quantification of [³²P]-labeled PL to LPS ratios in the OM (fractions 12–14) of WT and $\Delta tolQRA$ strains expressing TonBTM-TolA. Data are presented as mean \pm standard deviation from three independent replicates. **a–c** Two-sided Student's *t* tests were used to test for statistical significance; *P* value indicated was in comparison to WT with empty vector, unless otherwise specified. All strains here express additional copies of ExbBD from a pBAD33 vector.

membrane curvature locally, in a way that ultimately leads to proper invagination. In this regard, it is likely that other lipid transport processes may also play an unbeknownst role(s) in controlling septal membrane composition/curvature—an under-appreciated aspect of OM constriction during cell division. Future efforts should focus on elucidating the mechanisms of Tol-Pal function in OM lipid homeostasis and invagination.

Methods

Strains, plasmids, and growth conditions

List of *E. coli* strains used in this study can be found in Table S1. MG1655 strain expressing additional copies of ExbBD from pBAD33 vector was used as the wild-type strain for most experiments unless otherwise specified. W3110 strains expressing chromosomal Pal-mCherry from its native locus have been used in previous publications⁴⁰ and were acquired from the Duche laboratory. Gene deletion alleles were constructed using λ Red recombineering and transduced into relevant genetic background strains via P1 transduction^{64,65}. Strains were grown in Luria-Bertani (LB) broth (1% tryptone and 0.5% yeast extract, with or without 1% NaCl) supplemented with chloramphenicol (30 μ g/ml), ampicillin (100 μ g/ml), and/or 0.2% arabinose, to maintain plasmids or induce expression of ExbBD as needed. Agar plates contain 1.5% agar in the corresponding media. Cultures and plates were incubated at 37 °C unless otherwise specified. Plasmids expressing ExbBD, TonBTM-TolA, sfGFP-TonBTM-TolA, sfGFP-TolA, and sfGFP were constructed using Gibson assembly⁶⁶ (detailed in Supplementary Methods).

Efficiency of plating

Sensitivity towards SDS/EDTA, vancomycin, and low salt was tested by spotting serially diluted cultures of the respective strains onto agar plates with different conditions. When needed, agar plates were supplemented with chloramphenicol (30 μ g/ml) and ampicillin (100 μ g/ml) to maintain the plasmids and 0.2% arabinose to induce expression of ExbBD. Overnight cultures were 10-fold serially diluted

in 150 mM NaCl on 96-well plate. Two (for SDS/EDTA plates) or five μ l of each dilution were spotted onto the plates and incubated overnight at the indicated temperatures. All results shown are representative of at least three independent replicates.

Periplasmic RNase leakage assay

Overnight cultures of the indicated strains were pelleted, and the supernatant was filtered through a 0.22 μ m syringe filter. 10 μ l of filtered supernatant were spotted on an agar plate containing spectinomycin (of which the strains were sensitive) and 2 mg/ml yeast RNA. RNase leakages were visualized by overlaying cold 12.5% trichloroacetic acid onto the agar plates after overnight incubation at 37 °C. Clear zone indicates a lack of RNA and, therefore, the presence of RNase leakage into the culture supernatant.

Microscopy

To examine cellular morphology and fluorescence localization, overnight cultures were first diluted 1:2000 (1:1000 for LBON experiment) into fresh media. The sub-cultures were allowed to grow to mid-log (~4 h) before being concentrated 10-fold by centrifuging at 3000 $\times g$ for 5 min. 5 μ l of the concentrated cultures were spotted onto freshly made 1% agarose pad with the corresponding media. Images were acquired using a Zeiss LSM710 confocal microscope at $\times 100$ magnification and analyzed using ImageJ/Fiji (version 1.53c) and the MicrobeJ (version 5.131) plugin^{67,68}.

Quantification of OMV

Experiments to estimate OMV production had been previously described³³. Briefly, 10 ml cultures were grown in the presence of [¹⁴C]-acetate (final concentration of 0.2 μ Ci ml⁻¹; Perkin Elmer NEC084A001MC) until OD₆₀₀ reached ~0.5–0.7, after which the culture supernatants were collected and filtered through 0.45 μ m filters. The filtrates were ultracentrifuged, and the washed pellets (OMV) were measured for [¹⁴C] radioactive counts on a scintillation counter (MicroBeta2®, Perkin-Elmer). The relative quantity of OMV was presented

as the percentage of [^{14}C]-labeled lipids in the OMV relative to the total [^{14}C]-acetate labeling (cell pellet + OMV) of the respective strains.

PagP-mediated LPS hepta-acylation analysis

Experiment to quantify lipid asymmetry defects via measuring PagP-mediated lipid A palmitoylation (hepta-acylation) had been previously described^{14,69}. Briefly, 5 ml cultures were grown in the presence of [^{32}P]-phosphate (final concentration of $1\ \mu\text{Ci ml}^{-1}$; Perkin Elmer NEX060001MC) overnight, after which the cell pellets were harvested and washed twice with Tris-buffered saline (TBS). The pellet was resuspended in a single-phase Bligh/Dyer mixture, incubated for 20 min at room temperature, and centrifuged at $21,000 \times g$ for 30 min. The pellets containing LPS were washed once with 1 ml of single-phase Bligh/Dyer mixture and subsequently resuspended in 0.45 ml 12.5 mM sodium acetate containing 1% SDS (pH 4.5). The resuspension was sonicated for 15 min and heated at 100°C for 40 min. The mixtures were then converted into two-phase Bligh/Dyer mixture, and the lower phase (containing lipid A from hydrolyzed LPS) were collected and dried. The dried lipid A samples were resuspended in $30\ \mu\text{l}$ of chloroform/methanol mixture (4:1) for thin-layer chromatography (TLC) analysis using Silica Gel 60 F254 TLC plate (Merck Millipore) with the solvent system consisting of chloroform/pyridine/96% formic acid/water (50/50/14.6/4.6). A dried TLC plate was exposed to phosphor storage screens and visualized. Spots were quantified and averaged based on three independent experiments of lipid A isolation.

OM lipid composition analysis

Experiment to measure PL:LPS ratio at the OM had been previously described^{14,33,34}. Briefly, 10 ml cultures were grown in the presence of [^{32}P]-phosphate (final concentration of $1\ \mu\text{Ci ml}^{-1}$; Perkin Elmer NEX060001MC) until OD_{600} reached 1.5–2, after which the cell pellets were harvested and washed twice with TBS. Resulting cell pellets were re-suspended in 5 ml of 20% sucrose in 10 mM Tris-HCl pH 8.0 (w/w) containing 1 mM PMSF and $50\ \mu\text{g ml}^{-1}$ DNase I), and lysed by a single passage through a high-pressure French press (French Press G-M, Glen Mills) homogenizer at 8000 psi. Unbroken cells were removed by centrifugation at $3260 \times g$ for 10 min. The cell lysates were subjected to a two-step sucrose gradient ultracentrifugation to separate IM and OM fractions as previously described. OM fractions (fractions 12–14 out of 15 total fractions collected top-down) were pooled and concentrated for subsequent separation of PL and LPS. Protocol for the extraction of PLs and LPS had been described previously^{33,34}. Dried PLs were resuspended in $50\ \mu\text{l}$ of a mixture of chloroform:methanol (2:1); while dried LPS pellets were resuspended in $50\ \mu\text{l}$ 1% SDS. [^{32}P] radioactivity of equal volumes of PL or LPS solutions was measured using scintillation counting (MicroBeta2®, Perkin-Elmer). Scintillation counts of OM PLs were divided by the counts of OM LPS to obtain the PL/LPS ratio. The data shown is representative of three independent triplicate experiments.

Western blot

SDS-PAGE was performed using 12% Tris-HCl gels. Immunoblotting was performed by transferring from the gels onto polyvinylidene fluoride membranes (Immun-Blot® 0.2 μm , Bio-Rad) using the semi-dry electroblotting system (Trans-Blot® TurboTM Transfer System, Bio-Rad). Membranes were blocked using 1X casein blocking buffer (Sigma). Rabbit polyclonal α -TolA antisera was used at 1:1000 dilution. Rabbit polyclonal α -GFP was acquired from Abcam. Luminata Forte Western HRP Substrate (Merck Millipore) was used to develop the membranes, and chemiluminescent signals were visualized by G:BOX Chemi XT 4 (Genesys version 1.3.4.0, Syngene).

Reporting summary

Further information on research design is available in the Nature Portfolio Reporting Summary linked to this article.

Data availability

All data supporting the findings of this study are available within the paper and its supplementary files. Source data for main Figs. 3c, 4c, 5b, c, 6a–c, and supplemental Figs. S1–S4 are provided as a separate file. Source data are provided with this paper.

References

- Lundstedt, E., Kahne, D. & Ruiz, N. Assembly and maintenance of lipids at the bacterial outer membrane. *Chem. Rev.* **121**, 5098–5123 (2021).
- Yeow, J. & Chng, S.-S. Of zones, bridges and chaperones—phospholipid transport in bacterial outer membrane assembly and homeostasis. *Microbiology* **168**, 001177 (2022).
- Tan, W. B. & Chng, S.-S. How bacteria establish and maintain outer membrane lipid asymmetry. *Annu. Rev. Microbiol.* **78**, 553–573 (2024).
- Tomasek, D. & Kahne, D. The assembly of β -barrel outer membrane proteins. *Curr. Opin. Microbiol.* **60**, 16–23 (2021).
- Webby, M. N. et al. Lipids mediate supramolecular outer membrane protein assembly in bacteria. *Sci. Adv.* **8**, eadc9566 (2022).
- Rassam, P. et al. Supramolecular assemblies underpin turnover of outer membrane proteins in bacteria. *Nature* **523**, 333–336 (2015).
- Witwinowski, J. et al. An ancient divide in outer membrane tethering systems in bacteria suggests a mechanism for the diderm-to-monoderm transition. *Nat. Microbiol.* **7**, 411–422 (2022).
- Sandoz, K. M. et al. β -Barrel proteins tether the outer membrane in many Gram-negative bacteria. *Nat. Microbiol.* **6**, 19–26 (2021).
- Asmar, A. T. & Collet, J.-F. Lpp, the Braun lipoprotein, turns 50—major achievements and remaining issues. *FEMS Microbiol. Lett.* **365**, fny199 (2018).
- Okuda, S. & Tokuda, H. Lipoprotein sorting in bacteria. *Annu. Rev. Microbiol.* **65**, 239–259 (2011).
- Jones, N. C. & Osborn, M. Translocation of phospholipids between the outer and inner membranes of *Salmonella typhimurium*. *J. Biol. Chem.* **252**, 7405–7412 (1977).
- Donohue-Rolfe, A. M. & Schaechter, M. Translocation of phospholipids from the inner to the outer membrane of *Escherichia coli*. *Proc. Natl. Acad. Sci.* **77**, 1867–1871 (1980).
- Langley, K., Hawrot, E. & Kennedy, E. Membrane assembly: movement of phosphatidylserine between the cytoplasmic and outer membranes of *Escherichia coli*. *J. Bacteriol.* **152**, 1033–1041 (1982).
- Shrivastava, R., Jiang, X. E. & Chng, S. S. Outer membrane lipid homeostasis via retrograde phospholipid transport in *Escherichia coli*. *Mol. Microbiol.* **106**, 395–408 (2017).
- Douglass, M. V., McLean, A. B. & Trent, M. S. Absence of YhdP, TamB, and YdbH leads to defects in glycerophospholipid transport and cell morphology in Gram-negative bacteria. *PLoS Genet.* **18**, e1010096 (2022).
- Ruiz, N., Davis, R. M. & Kumar, S. YhdP, TamB, and YdbH are redundant but essential for growth and lipid homeostasis of the Gram-negative outer membrane. *MBio* **12**, e02714–e02721 (2021).
- Grimm, J. et al. The inner membrane protein YhdP modulates the rate of anterograde phospholipid flow in *Escherichia coli*. *Proc. Natl. Acad. Sci.* **117**, 26907–26914 (2020).
- Low, W. Y. & Chng, S. S. Current mechanistic understanding of intermembrane lipid trafficking important for maintenance of bacterial outer membrane lipid asymmetry. *Curr. Opin. Chem. Biol.* **65**, 163–171 (2021).
- Lloubès, R. et al. The Tol-Pal proteins of the *Escherichia coli* cell envelope: an energized system required for outer membrane integrity? *Res. Microbiol.* **152**, 523–529 (2001).
- Bernadac, A., Gavioli, M., Lazzaroni, J.-C. & Raina, S. & Lloubès, R. *Escherichia coli* tol-pal mutants form outer membrane vesicles. *J. Bacteriol.* **180**, 4872–4878 (1998).

21. Nagel de Zwaig, R. & Luria, S. E. Genetics and physiology of colicin-tolerant mutants of *Escherichia coli*. *J. Bacteriol.* **94**, 1112–1123 (1967).
22. Szczepaniak, J., Press, C. & Kleanthous, C. The multifarious roles of Tol-Pal in Gram-negative bacteria. *FEMS Microbiol. Rev.* **44**, 490–506 (2020).
23. Sturgis, J. N. Organisation and evolution of the tol-pal gene cluster. *J. Mol. Microbiol. Biotechnol.* **3**, 113–122 (2001).
24. Krachler, A. M., Sharma, A., Cauldwell, A., Papadakos, G. & Kleanthous, C. TolA modulates the oligomeric status of YbgF in the bacterial periplasm. *J. Mol. Biol.* **403**, 270–285 (2010).
25. Williams-Jones, D. P. et al. Tunable force transduction through the *Escherichia coli* cell envelope. *Proc. Natl Acad. Sci.* **120**, e2306707120 (2023).
26. Bonsor, D. A. et al. Allosteric β -propeller signalling in TolB and its manipulation by translocating colicins. *EMBO J.* **28**, 2846–2857 (2009).
27. Bouveret, E. et al. Peptidoglycan-associated lipoprotein-TolB interaction: a possible key to explaining the formation of contact sites between the inner and outer membranes of *Escherichia coli*. *J. Biol. Chem.* **270**, 11071–11077 (1995).
28. Bouveret, E., Bénédetti, H., Rigal, A., Loret, E. & Lazdunski, C. In vitro characterization of peptidoglycan-associated lipoprotein (PAL)-peptidoglycan and PAL-TolB interactions. *J. Bacteriol.* **181**, 6306–6311 (1999).
29. Parsons, L. M., Lin, F. & Orban, J. Peptidoglycan recognition by Pal, an outer membrane lipoprotein. *Biochemistry* **45**, 2122–2128 (2006).
30. Lazzaroni, J. C. & Portalier, R. The excC gene of *Escherichia coli* K-12 required for cell envelope integrity encodes the peptidoglycan-associated lipoprotein (PAL). *Mol. Microbiol.* **6**, 735–742 (1992).
31. Onodera, K., Rolfe, B. & Bernstein, A. Demonstration of missing membrane proteins in deletion mutants of *E. coli* K12. *Biochem. Biophys. Res. Commun.* **39**, 969–975 (1970).
32. Lopes, J., Gottfried, S. & Rothfield, L. Leakage of periplasmic enzymes by mutants of *Escherichia coli* and *Salmonella typhimurium*: isolation of “periplasmic leaky” mutants. *J. Bacteriol.* **109**, 520–525 (1972).
33. Jiang, X. E. et al. Mutations in enterobacterial common antigen biosynthesis restore outer membrane barrier function in *Escherichia coli* tol-pal mutants. *Mol. Microbiol.* **114**, 991–1005 (2020).
34. Tan, W. B. & Chng, S. S. Genetic interaction mapping highlights key roles of the Tol-Pal complex. *Mol. Microbiol.* **117**, 921–936 (2022).
35. Masilamani, R., Cian, M. B. & Dalebroux, Z. D. *Salmonella* Tol-Pal reduces outer membrane glycerophospholipid levels for envelope homeostasis and survival during bacteremia. *Infect. Immun.* **86**, e00173–18 (2018).
36. Gerding, M. A., Ogata, Y., Pecora, N. D., Niki, H. & De Boer, P. A. J. The trans-envelope Tol-Pal complex is part of the cell division machinery and required for proper outer-membrane invagination during cell constriction in *E. coli*. *Mol. Microbiol.* **63**, 1008–1025 (2007).
37. Meury, J. & Devilliers, G. Impairment of cell division in tolA mutants of *Escherichia coli* at low and high medium osmolarities. *Biol. Cell* **91**, 67–75 (1999).
38. Szczepaniak, J. et al. The lipoprotein Pal stabilises the bacterial outer membrane during constriction by a mobilisation-and-capture mechanism. *Nat. Commun.* **11**, 1305 (2020).
39. Yakhnina, A. A. & Bernhardt, T. G. The Tol-Pal system is required for peptidoglycan-cleaving enzymes to complete bacterial cell division. *Proc. Natl Acad. Sci.* **117**, 6777–6783 (2020).
40. Petit, M. et al. Tol energy-driven localization of Pal and anchoring to the peptidoglycan promote outer-membrane constriction. *J. Mol. Biol.* **431**, 3275–3288 (2019).
41. Hale, C. A., Persons, L. & de Boer, P. A. J. Recruitment of the TolA protein to cell constriction sites in *Escherichia coli* via three separate mechanisms, and a critical role for FtsWI activity in recruitment of both TolA and TolQ. *J. Bacteriol.* **204**, e00464–00421 (2022).
42. Gray, A. N. et al. Coordination of peptidoglycan synthesis and outer membrane constriction during *Escherichia coli* cell division. *elife* **4**, e07118 (2015).
43. Celia, H. et al. Structural insight into the role of the Ton complex in energy transduction. *Nature* **538**, 60–65 (2016).
44. Braun, V., Ratliff, A. C., Celia, H. & Buchanan, S. K. Energization of outer membrane transport by the ExbB ExbD molecular motor. *J. Bacteriol.* **205**, e00035–00023 (2023).
45. Hickman, S. J., Cooper, R. E., Bellucci, L., Paci, E. & Brockwell, D. J. Gating of TonB-dependent transporters by substrate-specific forced remodelling. *Nat. Commun.* **8**, 14804 (2017).
46. Ratliff, A. C., Buchanan, S. K. & Celia, H. The ton motor. *Front. Microbiol.* **13**, 852955 (2022).
47. Jordan, L. D. et al. Energy-dependent motion of TonB in the Gram-negative bacterial inner membrane. *Proc. Natl Acad. Sci.* **110**, 11553–11558 (2013).
48. Karlsson, M., Hannavy, K. & Higgins, C. F. A sequence-specific function for the N-terminal signal-like sequence of the TonB protein. *Mol. Microbiol.* **8**, 379–388 (1993).
49. Keller, K. L., Brinkman, K. K. & Larsen, R. A. In: *Methods in enzymology*. Vol. 423, 134–148 (Elsevier, 2007).
50. Kopp, D. R. & Postle, K. The intrinsically disordered region of ExbD is required for signal transduction. *J. Bacteriol.* **202**, e00687–19 (2020).
51. Braun, V. & Herrmann, C. Evolutionary relationship of uptake systems for biopolymers in *Escherichia coli*: cross-complementation between the TonB-ExbB-ExbD and the TolA-TolQ-TolR proteins. *Mol. Microbiol.* **8**, 261–268 (1993).
52. Lloubès, R., Goemaere, E., Zhang, X., Cascales, E. & Duché, D. Energetics of colicin import revealed by genetic cross-complementation between the Tol and Ton systems. *Biochem. Soc. Trans.* **40**, 1480–1485 (2012).
53. Samire, P. et al. Decoupling filamentous phage uptake and energy of the TolQRA motor in *Escherichia coli*. *J. Bacteriol.* **202** <https://doi.org/10.1128/jb.00428-19> (2020).
54. Chu, B. C., Peacock, R. S. & Vogel, H. J. Bioinformatic analysis of the TonB protein family. *Biometals* **20**, 467–483 (2007).
55. Larsen, R. A. et al. His20 provides the sole functionally significant side chain in the essential TonB transmembrane domain. *J. Bacteriol.* **189**, 2825–2833 (2007).
56. Ollis, A. A., Manning, M., Held, K. G. & Postle, K. Cytoplasmic membrane protonmotive force energizes periplasmic interactions between ExbD and TonB. *Mol. Microbiol.* **73**, 466–481 (2009).
57. Cascales, E., Bernadac, A., Gavioli, M., Lazzaroni, J.-C. & Lloubès, R. Pal lipoprotein of *Escherichia coli* plays a major role in outer membrane integrity. *J. Bacteriol.* **184**, 754–759 (2002).
58. Lazdunski, C. & Shapiro, B. M. Isolation and some properties of cell envelope altered mutants of *Escherichia coli*. *J. Bacteriol.* **111**, 495–498 (1972).
59. Paradis-Bleau, C. et al. Lipoprotein cofactors located in the outer membrane activate bacterial cell wall polymerases. *Cell* **143**, 1110–1120 (2010).
60. Egan, A. J. Bacterial outer membrane constriction. *Mol. Microbiol.* **107**, 676–687 (2018).
61. Alodaini, D. et al. Reduced peptidoglycan synthesis capacity impairs growth of *E. coli* at high salt concentration. *Mbio* **15**, e0032524 (2024).
62. Li, G.-W., Burkhardt, D., Gross, C. & Weissman, J. S. Quantifying absolute protein synthesis rates reveals principles underlying allocation of cellular resources. *Cell* **157**, 624–635 (2014).
63. Baccelli, P. et al. Timing of TolA and TolQ recruitment at the septum depends on the functionality of the Tol-Pal system. *J. Mol. Biol.* **434**, 167519 (2022).

64. Datsenko, K. A. & Wanner, B. L. One-step inactivation of chromosomal genes in *Escherichia coli* K-12 using PCR products. *Proc. Natl. Acad. Sci.* **97**, 6640–6645 (2000).
65. Baba, T. et al. Construction of *Escherichia coli* K-12 in-frame, single-gene knockout mutants: the Keio collection. *Mol. Syst. Biol.* **2**, 2006.0008 (2006).
66. Gibson, D. G. et al. Enzymatic assembly of DNA molecules up to several hundred kilobases. *Nat. Methods* **6**, 343–345 (2009).
67. Schindelin, J. et al. Fiji: an open-source platform for biological-image analysis. *Nat. Methods* **9**, 676–682 (2012).
68. Ducret, A., Quardokus, E. M. & Brun, Y. V. MicrobeJ, a tool for high throughput bacterial cell detection and quantitative analysis. *Nat. Microbiol.* **1**, 16077 (2016).
69. Chong, Z. S., Woo, W. F. & Chng, S. S. Osmoporin OmpC forms a complex with MlaA to maintain outer membrane lipid asymmetry in *Escherichia coli*. *Mol. Microbiol.* **98**, 1133–1146 (2015).
70. Wu, T. et al. Identification of a protein complex that assembles lipopolysaccharide in the outer membrane of *Escherichia coli*. *Proc. Natl. Acad. Sci.* **103**, 11754–11759 (2006).
71. Guzman, L.-M., Belin, D., Carson, M. J. & Beckwith, J. Tight regulation, modulation, and high-level expression by vectors containing the arabinose PBAD promoter. *J. Bacteriol.* **177**, 4121–4130 (1995).

Acknowledgements

We thank Denis Duché (CNRS, Aix-Marseille Université) for providing the W3110 *pal-mCherry* strains and the α -TolA antibody. This work was supported by the Singapore Ministry of Health National Medical Research Council under its Open Fund Individual Research Grant (MOH-000145) and the Singapore Ministry of Education Academic Research Fund Tier 1 grant (National University of Singapore-Faculty of Science Preparatory Grant Scheme) (both to S.-S.C.).

Author contributions

W.B.T. and S.-S.C. conceptualized the study, designed the experiments, and wrote the manuscript. W.B.T. performed the experiments and the initial data analysis.

Competing interests

The authors declare no competing interests.

Additional information

Supplementary information The online version contains supplementary material available at <https://doi.org/10.1038/s41467-025-57630-y>.

Correspondence and requests for materials should be addressed to Shu-Sin Chng.

Peer review information *Nature Communications* thanks the anonymous reviewers for their contribution to the peer review of this work. A peer review file is available.

Reprints and permissions information is available at <http://www.nature.com/reprints>

Publisher's note Springer Nature remains neutral with regard to jurisdictional claims in published maps and institutional affiliations.

Open Access This article is licensed under a Creative Commons Attribution-NonCommercial-NoDerivatives 4.0 International License, which permits any non-commercial use, sharing, distribution and reproduction in any medium or format, as long as you give appropriate credit to the original author(s) and the source, provide a link to the Creative Commons licence, and indicate if you modified the licensed material. You do not have permission under this licence to share adapted material derived from this article or parts of it. The images or other third party material in this article are included in the article's Creative Commons licence, unless indicated otherwise in a credit line to the material. If material is not included in the article's Creative Commons licence and your intended use is not permitted by statutory regulation or exceeds the permitted use, you will need to obtain permission directly from the copyright holder. To view a copy of this licence, visit <http://creativecommons.org/licenses/by-nc-nd/4.0/>.

© The Author(s) 2025